Determination of the Acid Strength of Binary Oxide Catalysts Using Temperature-Programmed Desorption of Pyridine

Atsushi Satsuma,* Yenni Westi, Yuichi Kamiya, Tadashi Hattori, and Yuichi Murakami#

Department of Applied Chemistry, School of Engineering, Nagoya University, Furo-cho, Chikusa-ku, Nagoya 464-01

(Received December 12, 1996)

The temperature-programmed desorption of pyridine (Py-TPD) was performed for measuring the acid strength and acid amount of binary oxide catalysts. First, the optimum measurement conditions were determined by comparing the TPD spectra with the infrared spectra of adsorbed pyridine measured under the same conditions in order to minimize the shift in the desorption temperature and contribution of physically absorbed and/or weakly held pyridine. The following conditions were found to be optimum: purging at 423 K for 2 h, *W/F* (*W*, sample weight; *F*, flow rate of the carrier) of 100 mg/150 cm ^{3} min $^{-1}$, and a heating rate of 5 K min^{-1}. This method was applied then to a series of binary mixed oxide catalysts. The amount of desorbed pyridine was 15—24% of the full coverage of pyridine on the catalyst surface with few exceptions. The highest acid strength, determined from the Py-TPD spectra, was well-correlated to that determined from a color change of Hammett indicators. The potential of the Py-TPD for determining the acid strength and the acid amount on binary oxide catalysts is discussed.

There is significant motivation to gain a better understanding of the acidic properties of metal oxide catalysts, since it is well-known that the catalytic activity and selectivity frequently depend on acidic properties of catalysts. Measurements of the acidic properties, i.e., the acid strength and acid amount, are important, and a reliable method to characterize the acidic properties is desired. Many techniques have been used to measure the acidic properties of solid acid catalysts, such as, Hammett indicators,[1—3] a microcalorimeter,[4,5] infrared spectroscopy,[6] test reactions,[7] and the temperature-programmed desorption (TPD) of probe molecules.[8—13] Since the temperature-programmed desorption of chemisorbed basic molecules is an easy and reproducible method for determining the acid amount of solid catalysts as well as the acid strength, it is used frequently. Ammonia is widely used as a gaseous probe molecule because of its small molecular size, stability and strong basicity ($pK_a = 9.2$). Although the molecular size of pyridine is large, the lower basicity ($pK_a = 5.2$) may enable one to easily measure strong acids, such as solid superacids,[13] and a high sensitivity can be expected in the detection of pyridine using a flame-ionization detector (FID).

TPD of pyridine (Py-TPD) for the acid-strength characterization of oxide catalysts has been reported by several authors. Kojima et al.[11] have studied Py-TPD of ion-exchanged mordenites, and Karge et al.[12] have also studied Py-TPD of dealuminated Y-zeolites. Since they found that the steric factor plays a dominant role in the case of Py-TPD from zeolites, the application of Py-TPD to porous crystals seems to be difficult. Matsuhashi et al.[13] have reported on Py-TPD for determining the acid strength of solid superacids by using thermogravimetrical and differential thermal analyses methods, which showed that there is a linear relation between the H_0 values of the highest acid strength ($H_{0,max}$) determined by the Hammett method and the termination temperature of pyridine desorption.

The TPD method usually depends greatly on the experimental conditions. For determining the acid strength, readsorption of the probe molecules in the sample bed should be minimized during the measurement, because it results in a shift of the desorption temperature.[9,10] For determining the acid amount, the contribution of physically adsorbed molecules on the spectra should be minimized. Thus, the measurement conditions for Py-TPD must be strictly examined. In this study, in order to establish the Py-TPD method for measuring the acid strength and the acid amount of binary mixed oxide catalysts, the experimental conditions of Py-TPD, i.e., purging temperature, contact time and heating rate, were carefully examined by comparing the TPD spectra with the IR spectra of the adsorbed pyridine. Then, the acid strength and the acid amount determined from Py-TPD were respectively considered based on the highest H_0 values determined by the Hammett indicators and the surface area.

Experimental

Catalysts. The binary mixed oxides used in this study are listed in Table 1. Some of them were prepared by a coprecipitation method or a sol–gel method[14] using the precursors shown in the table. In the coprecipitation method, the precursors were dissolved in hydrochloric acid or ethanol. Two solutions containing precursors were mixed well using a magnetic stirrer. The mixed metal hydroxides were then precipitated by adding an excess amount of an aqueous

Present address: Aichi Institute of Technology, Yagusa, Toyota 470-03, Japan.

Table 1. Binary Mixed Oxides and Precursors Used for This Study

Catalyst	Name	Molar ratio (oxide/oxide)	Source or preparation method	Precursor
SiO_2–Al_2O_3	Si–Al(1)	1–0.24	JRC-SAH-1[a)]	
SiO_2–Al_2O_3	Si–Al(2)	1–0.1	JRC-SAL-2[a)]	
SiO_2–MgO	Si–Mg(1)	1–0.65	JRC-SM-1[a)]	
SiO_2–MgO	Si–Mg(2)	1–1	Sol–gel	$Mg(CH_3COO)_2$–$(C_2H_5O)_4Si$
SiO_2–TiO_2	Si–Ti	1–1	Nikki[b)]	
SiO_2–ZnO_2	Si–Zn	1–0.4	Nikki[b)]	
Al_2O_3–SnO_2	Al–Sn	1–1	Sol–gel	$Al[OCH_3(CH_3)_2]_3$–$SnCl_2(acac)_2$
Al_2O_3–ZrO_2	Al–Zr	1–1	Co-precipitation	$Al[OCH_3(CH_3)_2]_3$–$ZrO(CH_3COO)_2$
MgO–SnO_2	Mg–Sn	1–1	Sol–gel	$Mg(CH_3COO)_2$–$SnCl_2(acac)_2$
MgO–ZrO_2	Mg–Zr	1–1	Sol–gel	$Mg(CH_3COO)_2$–$ZrO(CH_3COO)_2$
MgO–Al_2O_3	Mg–Al	1–1	Sol–gel	$Mg(CH_3COO)_2$–$Al[OCH_3(CH_3)_2]_3$
ZrO_2–Bi_2O_3	Zr–Bi	1–1	Co-precipitation	$ZrO(CH_3COO)_2$–$BiCl_3$
SnO_2–Bi_2O_3	Sn–Bi	1–1	Co-precipitation	$SnCl_2(acac)_2$–$BiCl_3$
SiO_2–Bi_2O_3	Si–Bi	1–1	Co-precipitation	$(C_2H_5)_4SiO_2$–$BiCl_3$

a) Supplied from the Committee on Reference Catalyst of the Catalyst Society of Japan. b) Supplied from Nikki Chemical Japan.

ammonia solution. After filtration, the precipitates were carefully washed, dried at 400 K in an oven for about 8 h, and finally calcined at 773 K for about 5 h in air. In the sol–gel method, each precursor was solved separately in ethanol at room temperature. Two ethanol solutions containing a precursor were mixed well; then, water was slowly added to the solution using a microtube-pump at a rate of 100 $cm^3 min^{-1}$. After the solution became viscous and gelatinized, the gelatin was dried under reduced pressure by using an evaporator, followed by calcination at 773 K for about 18 h in flowing oxygen. Silica was supplied from the Committee on Reference Catalysts of the Catalyst Society of Japan (JRC-SIO-8).

Visual Color Change in Hammett Indicators. A measurement of the $H_{o,max}$ values was conducted using Hammett indicators.[1,2] After calcination of about 10 mg of the catalyst at 673 K for 3 h, benzene containing the Hammett indicator was added at room temperature. The acid strength was determined on the basis of the color-change pattern of the Hammett indicators adsorbed on the surface.

Temperature-Programmed Desorption of Pyridine (Py-TPD). The temperature-programmed desorption of pyridine (Py-TPD) was performed using the apparatus shown in Fig. 1. A U-shape tube made of quartz was used as the sample cell. Then, 100 mg of the catalyst was placed in a sample cell and preheated at 673 K for two hours in flowing helium. After cooling to the prescribed temperature in a stream of helium, the catalyst was exposed to a flow of 2 mol% of pyridine diluted in helium with a flow rate of 150 cm^3 min^{-1} for 30 min. The equilibrium adsorption was confirmed from the concentration of pyridine passed though the catalyst. Then, the system was kept at the same temperature for two hours in flowing helium in order to purge any excess and/or weakly held pyridine. Finally, the TPD measurement was performed from the purging temperature to 1073 K at a heating rate of 5 K min^{-1}. The desorbed pyridine was detected with a flame-ionization detector (FID) because of the high sensitivity to organic molecules and no influence by water vapor. The line between the sample cell and the FID was kept at 400 K. In a separate experiment, desorbed molecules from Si–Al(2) catalyst were analyzed. Only pyridine was detected in the desorption stream, and no decomposed or polymerized products were detected.

The temperature at which pyridine desorption terminated (hereafter called as "T-end") was used as a measure of the highest acid strength. T-end was defined as the highest temperature at which the slope of the FID response became zero, and was determined from the highest cross-section temperature of the first-differential and the second-differential curve of the desorption spectrum. The error in the determination of T-end was within 5 K.

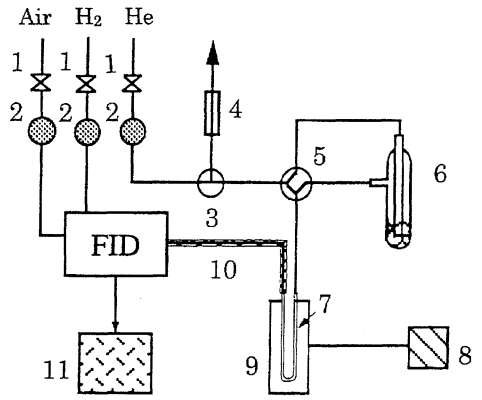

Fig. 1. Flow diagram of Py-TPD experiment. (1) stop valve, (2) flow controller, (3) three-way valve, (4) soap film meter, (5) four-way valve, (6) pyridine saturator, (7) U-shape tube and sample (8) temperature controller, (9) electric furnace, (10) flexible heater kept at 400 K, and (11) recorder.

Infrared Spectra of Adsorbed Pyridine. The infrared spectra were measured with JASCO FT/IR-300 equipped with a quartz cell and a flow system similar to that use in the Py-TPD measurement. A catalyst (40 mg) was pressed into a disk and placed in a quartz cell. The sample was heated at 673 K for two hours in flowing oxygen. After cooling to a prescribed temperature, 5 mm^3 of pyridine was injected into a stream of helium at a flow rate of 150 cm^3 min^{-1}. Then, the infrared spectra were taken at various purging times from 0 to 120 min in flowing helium.

Results and Discussion

1. Experimental Conditions in Py-TPD Measurements. 1.1 Purging Temperature. Figure 2 shows the Py-TPD spectra from silica with various purging temperatures. When the purging temperature of pyridine was 373 K, a sharp spec-

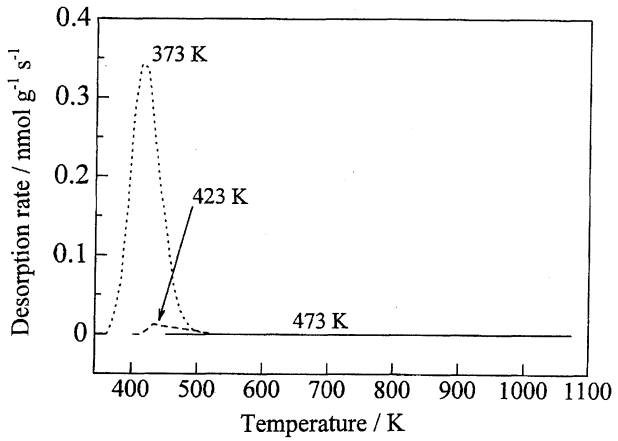

Fig. 2. Py-TPD spectra from silica with various purging temperatures.

trum of desorbed pyridine was observed with an amount of 0.024 mmol g^{-1}. When the purging temperature was increased to 423 K, the spectrum showed a small broad peak, and the desorbed amount decreased to 0.0015 mmol g^{-1}. It is worth noting that the Py-TPD spectra showed a straight baseline having a high signal/noise ratio, and that this method is very sensitive for detecting desorbed pyridine. The desorption of pyridine was not detected when purging was carried out at 473 K.

Figure 3 shows the IR spectra of adsorbed pyridine on silica with various purging temperatures. In the IR spectrum at 373 K, the absorption bands were observed at 1594 and 1444 cm^{-1}, and were assignable to hydrogen-bonded and/or coordinatively held pyridine.[15,16] There was also observed a shoulder peak at 1575 cm^{-1} assignable to hydrogen-bonded pyridine.[15—17] These bands were significantly decreased by purging with flowing helium; no adsorption band could be observed after purging at 423 and 473 K. These results

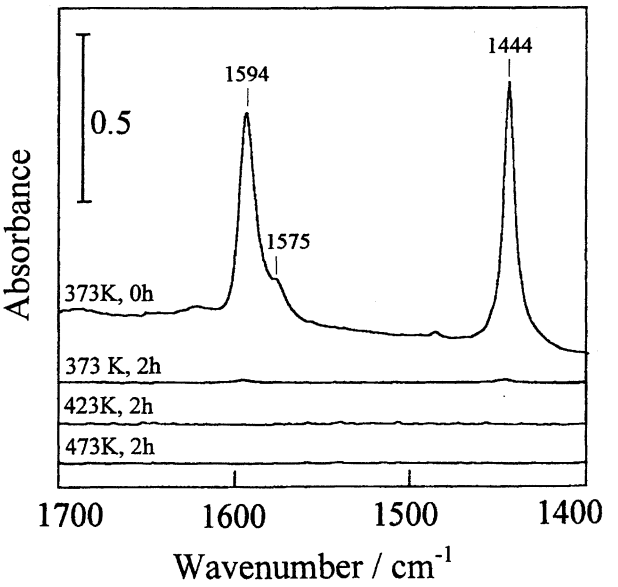

Fig. 3. IR spectra of adsorbed pyridine on silica with various purging temperatures.

suggest that these bands can be attributable to physically adsorbed and/or weakly held pyridine on the silica surface. Since the silica surface is generally considered to be inert, the results observed in the IR spectra are reasonable.

A comparison between Figs. 2 and 3 indicates that the Py-TPD spectra from silica should be due to physically adsorbed and/or weakly held pyridine. After purging at 373 K, a detectable amount of absorbed pyridine was observed in both the IR and TPD spectra. After purging at 423 K, pyridine was not detected in IR, and only a small desorption peak was observed in TPD. The amount of desorbed pyridine in TPD was less than 0.004 molecule nm^{-2} at 423 K, which was only 0.14% coverage over the silica surface. Therefore, it can be said that physically adsorbed pyridine is practically removed by purging at 423 K for 2 h.

Figure 4 shows the Py-TPD spectra from Si–Mg(1) at various purging temperatures. The spectrum after purging at 373 K showed a sharp peak with a desorption maximum at about 460 K, and pyridine desorption terminated (T-end) at 838 K. T-end was determined from the highest cross-section temperature of the first-differential and the second-differential curve of the desorption spectrum. The higher purging temperature resulted in a shift of this peak maximum to a higher temperature. However, the figure of the spectra at higher temperature, above 650 K, and T-end did not vary with the purging temperature.

Figure 5 shows the IR spectra of the adsorbed pyridine on Si–Mg(1) with various purging temperatures. When pyridine was purged at 373 K for 2 h, the absorption bands were observed at 1444, 1491, 1546, 1575, 1607, and 1638 cm^{-1} together with a shoulder at 1596 cm^{-1}. All of the bands decreased after purging at 423 K, especially the shoulder at 1596 cm^{-1} disappeared at 423 K. Since this band was assigned to physically adsorbed pyridine in the case of silica, the result indicates the selective elimination of physically adsorbed pyridine. The other bands can be attributable to pyridine coordinated to Lewis acid (LPy) at 1444, 1491, 1575, and 1607 cm^{-1}, and pyridine adsorbed on Brønsted acid (BPy) at 1491, 1546, 1575, and 1638 cm^{-1}.[15,16] These results indicate that Py-TPD spectrum from Si–Mg(1) af-

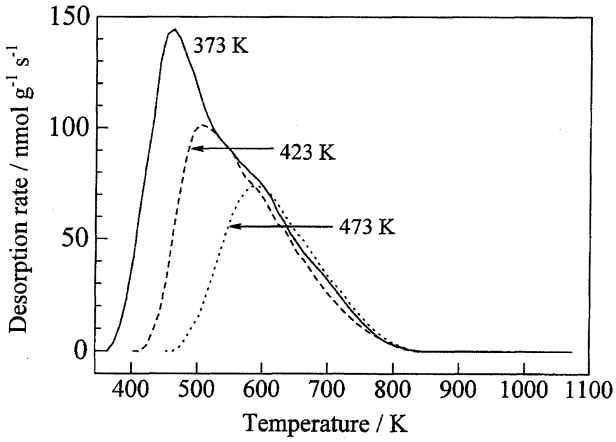

Fig. 4. Py-TPD spectra from Si–Mg(1) with various purging temperatures.

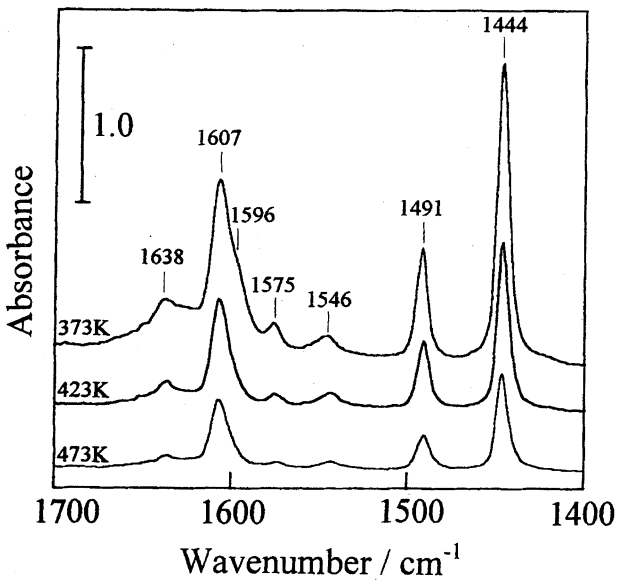

Fig. 5. IR spectra of adsorbed pyridine on Si–Mg(1) with various purging temperatures for 2 h.

ter purging at 373 K contained both physically adsorbed and chemisorbed pyridine, and that purging above 423 K eliminated the contribution of physically adsorbed pyridine. However, the purging at 473 K removed not only physically adsorbed pyridine, but also some of the chemisorbed pyridine. Thus, it can be concluded that purging at 423 K is practically sufficient for eliminating physically adsorbed pyridine in a Py-TPD measurement. It is known that physically adsorbed pyridine can be removed by evacuation at 423 K, as Parry reported.[18] Although pyridine was purged in flowing He in this study, the purging temperature for removing physically adsorbed pyridine agreed with that in the vacuum system.

As shown in Figs. 2 and 4, the temperature at which the maximum desorption rate was observed (T-max) was varied significantly with the purging temperature. Typical results are shown in Fig. 4; i.e., T-max was markedly shifted to higher temperatures along with an increase in the purging temperature. However, the effect of the purging temperature was not significant on the desorption spectrum at a high-temperature region, especially at the temperature at which the desorption terminated (T-end). Although the purging temperature was varied from 373 to 473 K, the shift of T-end on Si–Mg(1) was only less than 5 K. This result shows the high reproducibility and reliability of T-end.

1.2 Contact Time. Figure 6 shows the Py-TPD spectra from Si–Mg(1) with various contact times, i.e., W/F (W, sample weight; F, flow rate of the carrier). The experiment was performed by varying the catalyst weight of Si–Mg-(1), while the flow rate of the carrier gas was fixed at 150 $cm^3\ min^{-1}$. The desorption spectrum having T-end at 898 K was observed at a catalyst weight of 1000 mg. When the catalyst weight was decreased to 100 mg, T-end was observed at a lower temperature, i.e., 833 K, and the desorption peak became slightly smaller. A similar desorption spectrum was

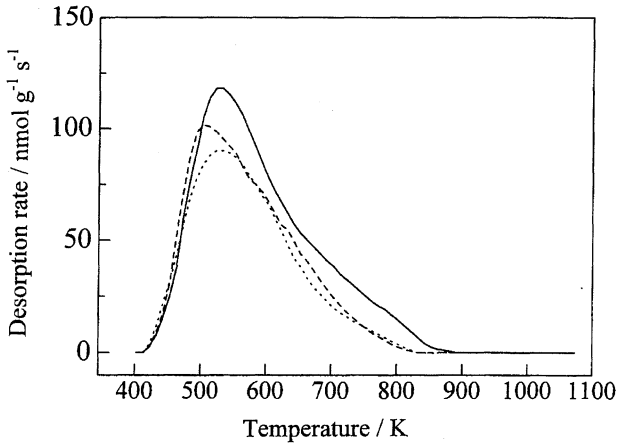

Fig. 6. Py-TPD spectra from Si–Mg(1) with various contact times. Flow rate of carrier gas was fixed at 150 $cm^3\ min^{-1}$ and catalysts weight was varied at (·····) 10 mg, (- - -) 100 mg, and (—) 1000 mg.

obtained upon a further decrease in the catalyst weight to 10 mg, i.e., a further decrease in the contact time did not significantly affect T-end and the desorbed amount of pyridine. In the case of TPD of ammonia with freely occurring readsorption, a shift in the desorption peak was observed by Niwa et al.[9,10] A larger W/F resulted in a higher desorption temperature. In the case of Py-TPD, T-end also shifted to a higher temperature when 1000 mg of the catalyst was used. However, since an increase in the amount of desorbed pyridine was also observed, the shift of T-end may have been due to insufficient purging of physically adsorbed and/or weakly held pyridine. Because the spectra at 100 mg was very similar to that at 10 mg, as observed in the figure, the pyridine was sufficiently purged, and the effect of readsorption was small in the case of a catalyst weight less than 100 mg. Thus, 100 mg was selected as the standard catalyst amount for a helium flow rate of 150 $cm^3\ min^{-1}$.

1.3 Heating Rate. Figure 7 shows the Py-TPD spectra from Si–Mg(1) for various heating rates. For heating rates at 2.5, 5, and 10 K min^{-1}, T-end was at 828, 833, and 863 K, and the desorbed amounts of pyridine were 0.231, 0.240,

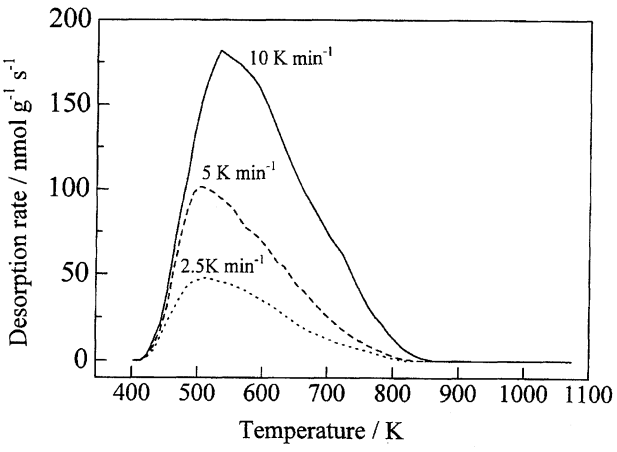

Fig. 7. Py-TPD spectra from Si–Mg(1) with various heating rates.

and 0.227 mmol g^{-1}, respectively. The amount of desorbed pyridine was not seriously affected by the heating rate, and the error in the desorbed amount was about 5%. On the other hand, the heating rate had an effect on T-end. In the spectrum measured at 10 K min^{-1}, T-end was 30 K higher than those measured at a lower heating rate. However, in the cases of 2.5 and 5 K min^{-1}, the differences in the T-end was within 5 K. Thus, the heating rate was selected to be 5 K min^{-1} as the standard condition.

1.4 Estimation of the Acid Strength and Acid Amount from Py-TPD. In the Py-TPD spectra, the temperature of desorption should stand for the acid strength. Since T-max was strongly affected by the purging temperature, and easily shifted along with a variation in the contact time, further optimization of the experimental conditions should be necessary in order to use of T-max as a measure of the acid strength. When adsorbed pyridine was sufficiently purged, and the heating rate was slow enough, the termination temperature of desorption, T-end, was hardly affected by the experimental conditions, i.e., the purging temperature, contact time and heating rate. This demonstrated that the value of T-end is reliable as a measure of the highest strength of acid sites.

The desorbed amount of pyridine should stand for the acid amount of the catalyst. The amount of desorbed pyridine strongly depended on the purging temperature. However, when physically adsorbed and/or weakly held pyridine was sufficiently removed, the Py-TPD spectra showed a constant amount of the desorbed pyridine, being independent of the contact time and heating rate. This suggests the possibility to measure the amount of acid sites stronger than a certain level.

In the following section, T-end and the amount of desorbed pyridine of various binary oxide catalysts are compared.

2. Py-TPD Spectra from Various Binary Oxides. 2.1 Classification of the Py-TPD Spectra from Binary Oxide Catalysts. As shown in Fig. 8, the TPD spectra from binary oxide catalysts were classified into three types: Single symmetrical peak at low temperature (type I), single broad and asymmetrical peak around a middle temperature (type II), and double peaks at low and high temperature (type III). Figure 8 shows typical examples. Mg–Al gave a spectrum of type I: Only a sharp peak was observed at low temperature, and the desorption terminated (T-end) at 563 K. The spectrum from Si–Mg(2) was a typical example of type II: The peak was broader and T-end was higher than 800 K. A typical example of type III was obtained from Si–Al(2): The spectrum has two peak maxima at 503 and 813 K, and T-end was 973 K.

The type of spectrum, the acid amount, T-max and T-end of all the catalysts are summarized in Table 2. $H_{o,max}$, determined from Hammett indicators, is also summarized in the table. As shown, $H_{o,max}$ and the type of spectrum were well-correlated to each other, i.e., $H_{o,max}$ ranged from −11.99 to −8.2 for type-III catalysts, from −8.2 to +1.5 for type-II catalysts and +4.8 for type-I catalysts. Thus, the classification of the type of spectrum is also a classification

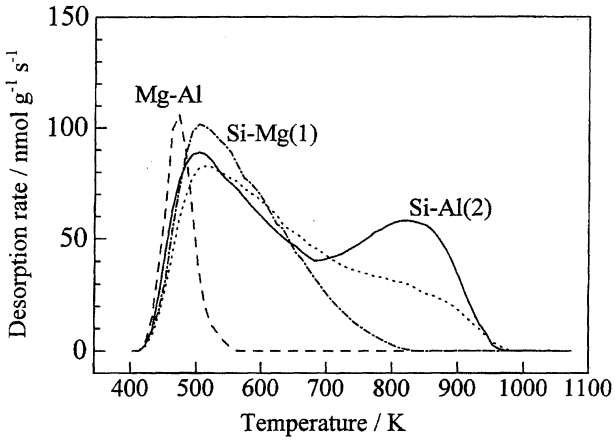

Fig. 8. Py-TPD spectra of (- - -) Mg–Al, (–•–) Si–Mg(1), and (——) Si–Al(2) measured after preheating at 673 K. Py-TPD spectrum of Si–Al(2) was also measured after preheating at 873 K (·····).

of the acid strength into three types: Those catalysts having very strong acid sites (type III), medium acid sites (type II), and only weak acid sites (type I).

2.2 Acid Amount. As shown in Table 2, most of the desorbed amount of pyridine was in the range of 0.4—0.7 molecule per nm^2, except for Mg–Al, Sn–Bi, and Si–Bi. This amount corresponds to 15—24% of the surface coverage, since the theoretical surface concentration of pyridine at full coverage is 2.8 molecules per nm^2, which was calculated on the basis of the van der Waals diameter and the closest packing of end-on pyridine. Hashimoto reported that the acid sites of Si–Al(2) stronger than $H_o = -3.0$, measured by butylamine titration, is 0.96 molecule per nm^2 and 0.50 molecule per nm^2 by the Hammett indicator adsorption method.[19,20] The acid amount of the same catalyst measured in this study, i.e., 0.44 molecule per nm^2, was close to that measured by the Hammett indicator adsorption method, rather than that by butylamine titration. The difference in the measured acid amount may have been due to a steric hindrance or a difference in the basicity of the probe molecules. However, since the surface coverage of pyridine was lower than 25%, the former is not the reason. Since butylamine ($pK_a = 10.6$) is a stronger base than pyridine ($pK_a = 5.2$), it can be expected that the lower acid amount measured by the Py-TPD was due to the weaker adsorption of pyridine, resulting from the difference in the basicity of the probe molecules.

2.3 Acid Strength. As shown in Table 2, T-end and $H_{o,max}$ of binary oxides were almost in the same sequence. Although T-max was fairly correlated with $H_{o,max}$, it varied over a narrow rage of temperature, 453—503 K, suggesting that T-max in the Py-TPD spectrum is not sensitive to the acid strength. Figure 9 shows the correlation between the reciprocal temperature at which pyridine desorption terminated ($1/T$-end) and the $-H_{o,max}$ values measured by Hammett indicators. A good correlation was observed, strongly indicating that the Py-TPD measurement is effective for determining the acid strength of binary oxide catalysts. This agrees qualitatively with the result reported by Matsuhashi et

Table 2. Acid Strength and Acid Amount of Binary Oxides

Catalyst	$H_{o,max}$	Surface area	Type of	Acid amount		T-max	T-end
		$m^2\ g^{-1}$	spectrum	$mmol\ g^{-1}$	molecule per nm^2	K	K
Si–Al(2)	−11.99	560.0	III	0.412	0.44	503	973
Si–Al(1)	−11.99	511.0	III	0.357	0.42	483	943
Si–Ti	−8.2	186.6	III	0.188	0.61	503	893
Si–Mg(1)	−8.2	450.3	II	0.240	0.54	503	833
Al–Sn	−8.2	115.5	II	0.112	0.58	473	773
Al–Zr	−5.6	214.9	II	0.239	0.67	474	753
Si–Mg(2)	−5.6	76.7	II	0.064	0.50	473	723
Si–Zn	−3.0	91.5	II	0.072	0.47	483	753
Mg–Sn	−3.0	44.6	II	0.050	0.68	483	643
Mg–Zr	+1.5	82.7	II	0.079	0.57	483	623
Zr–Bi	+1.5	18.5	II	0.020	0.65	463	583
Mg–Al	+4.8	200.4	I	0.053	0.16	473	563
Sn–Bi	+4.8	64.8	I	0.014	0.13	473	543
Si–Bi	+4.8	67.0	I	0.004	0.036	453	523

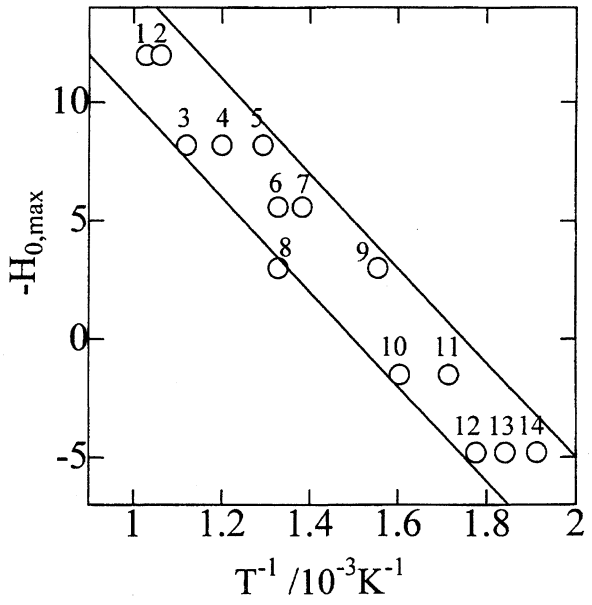

Fig. 9. Correlation between T-end and $H_{o,max}$ values of (1) Si–Al(2), (2) Si–Al(1), (3)Si–Ti, (4) Si–Mg(1), (5) Al–Sn, (6) Al–Zr, (7) Si–Mg(2), (8) Si–Zn, (9) Mg–Sn, (10) Mg–Zr, (11) Zn–Bi, (12) Mg–Al, (13) Sn–Bi, and (14) Si–Bi.

al.,[13] though they preferred a plot of $-H_{o,max}$ against T-end, but not $1/T$-end. However, T-end observed in this study was significantly higher compared with that which Matsuhashi et al. reported. For example, T-end of Si–Al(2) was at 973 K in this study, while it was at 690 K in their result. Since T-end in their result was similar to the termination temperature of a lower peak in this study, the difference may be due to a contribution of the higher peak concerning strong acid sites. The samples were pretreated in flowing helium in our study, while they heated the samples under a vacuum; the latter is widely accepted to strongly activate acid sites. One possibility is the decomposition or polymerization of pyridine, which was not observed in the IR spectra and gaschromatography in the standard conditions of the present study. Another is the irreversible adsorption of pyridine on strongly activated acid sites. As shown in Fig. 8, the higher peak was significantly decreased when Si–Al(2) was preheated in helium at 873 K, which was higher by 200 K than the standard conditions. It can be expected that the lower T-end in Matsuhashi's result is also due to a difference in the pretreatment, i.e., pyridine may be irreversibly adsorbed on the acid sites strongly activated under a vacuum.

Conclusion

The potential of Py-TPD for determining the acid strength and acid amount of binary oxide catalysts was discussed by comparing with the IR spectra and $H_{o,max}$, determined from Hammett indicators. From the results obtained in the present study, it was demonstrated that the Py-TPD measurement is effective for determining the acid strength of binary oxide catalysts.

1. The optimum measurement conditions for the Py-TPD experiment were determined in order to obtain a measurement of the Py-TPD spectra with a minimum shift of the desorption temperature and a minimum contribution of physically adsorbed and/or weakly held pyridine, and were recommended as follows: purging temperature, 423 K; catalyst weight, 100 mg for helium flow rate of 150 $cm^3\ min^{-1}$; heating rate, 5 $K\ min^{-1}$.

2. The termination temperature of desorption, T-end, can be a measure of the highest strength of acid sites, since a good correlation was obtained between the reciprocal temperature of the termination ($1/T$-end) in the Py-TPD spectra and the $H_{o,max}$ values determined by the Hammett indicators.

3. The amount of desorbed pyridine measured under the present conditions was 15—24% of the full coverage of pyridine on the catalyst surface. Although the result on Si–Al-(2) agreed with that measured by the Hammett indicator adsorption method, it was about one-half of that measured by butylamine titration.

This work was partly supported by a Grant-in-Aid (No. 08750907) from the Ministry of Education, Science, Sports and Culture.

References

1) K. Tanabe, "Solid Acids and Bases—Their Catalytic Properties," Kodansha, Tokyo, Academic Press, New York (1970).
2) K. Tanabe, M. Misono, Y. Ono, and H. Hattori, "New Solid Acids and Bases," Kodansha–Elsevier, Tokyo (1989).
3) K. R. P. Sabu, K. V. C. Rao, and C. G. R. Nair, *Bull. Chem. Soc. Jpn.*, **64**, 1920 (1991).
4) N. Cardona-Martinez and J. A. Dumesic, *J. Catal.*, **125**, 427 (1990).
5) N. Cardona-Martinez and J. A. Dumesic, *Adv. Catal.*, **38**, 149 (1992).
6) C. U. I. Odenbrand, J. G. M. Brandin, and G. Busca, *J. Catal.*, **135**, 505 (1992).
7) T. A. Andres, J. M. Arandes, M. Olazar, and J. Bilbao, *Ind. Eng. Chem. Res.*, **29**, 1172 (1990).
8) R. J. Cvetanovic and Y. Amenomiya, *Adv. Catal.*, **17**, 103 (1967).
9) M. Niwa, M. Iwamoto, and K. Segawa, *Bull. Chem. Soc. Jpn.*, **59**, 3735 (1986).
10) M. Niwa, N. Katada, M. Sawa, and Y. Murakami, *J. Phys. Chem.*, **99**, 8812 (1995).
11) M. Kojima, M. W. Rautenbach, and C. T. O'Connor, *J. Catal.*, **112**, 495 (1988).
12) H. G. Karge, V. Dondur, and T. Weitkamp, *J. Phys. Chem.*, **95**, 283 (1991).
13) H. Matsuhashi, H. Motoi, and K. Arata, *Catal. Lett.*, **26**, 325 (1994).
14) T. Hattori, S. Kito, H. Niwa, Y. Westi, A. Satsuma, and Y. Murakami, *Stud. Surf. Sci. Catal.*, **90**, 229 (1994).
15) H. Knözinger, *Adv. Catal.*, **25**, 184 (1976).
16) H. Knözinger and P. Ratnasamy, *Catal. Rev. Sci. Eng.*, **17**, 31 (1978).
17) C. Morterra, S. Coluccia, A. Chiorino, and F. Boccuaai, *J. Catal.*, **54**, 348 (1978).
18) E. P. Parry, *J. Catal.*, **2**, 371 (1963).
19) K. Hashimoto, T. Masuda, H. Motoyama, H. Yakushiji, and M. Ono, *Ind. Eng. Chem. Prod. Res. Dev.*, **25**, 243 (1986).
20) K. Hashimoto, T. Masuda, H. Ueda, and N. Kitano, *Appl. Catal.*, **22**, 147 (1986).